Dalton Transactions

Correlating Magnetic Anisotropy and [Mo(CN)7]4- Geometry of MnII-MoIII Magnetic Frameworks

Journal:	*Dalton Transactions*
Manuscript ID	DT-ART-05-2019-002164.R1
Article Type:	Paper
Date Submitted by the Author:	23-Jun-2019
Complete List of Authors:	Magott, Michal; Jagiellonian University, Faculty of Chemistry Dunbar, Kim; Texas A and M University, Chemistry Pinkowicz, Dawid; Jagiellonian University, Faculty of Chemistry

Journal Name

ARTICLE

Correlating Magnetic Anisotropy and $[Mo(CN)_7]^{4-}$ Geometry of Mn^{II}-Mo^{III} Magnetic Frameworks

Received 00th January 20xx,
Accepted 00th January 20xx

DOI: 10.1039/x0xx00000x

www.rsc.org/

Michał Magott,[a] Kim R. Dunbar*[b] and Dawid Pinkowicz*[a]

Four new three-dimensional (3-D) coordination frameworks based on the heptacyanomolybdate(III) anion were prepared and characterised by magnetic measurements: $\{[Mn^{II}(imH)_2]_2[Mn^{II}(H_2O)(imH)_3][Mn^{II}(imH)_4][Mo^{III}(CN)_7]_2{\cdot}6H_2O\}_n$ (**1**) (imH = imidazole), $\{[Mn^{II}(H_2O)_2(imH)]_3[Mn^{II}(H_2O)(imH)_2][Mo^{III}(CN)_7]_2{\cdot}5H_2O\}_n$ (**2**), $\{[Mn^{II}(Htrz)(H_2O)_2][Mn^{II}(Htrz)_{0.7}(H_2O)_{2.3}][Mo^{III}(CN)_7]{\cdot}5.6H_2O\}_n$ (**3**) (Htrz = 1,2,4-triazole) and $\{[Mn^{II}(H_2O)_2]_3[Mn^{II}(H_2O)_4][Mo^{III}(CN)_7]_2{\cdot}6H_2O{\cdot}2urea\}_n$ (**4**). All four compounds exhibit long-range ferrimagnetic ordering and exhibit an opening of their magnetic hysteresis loops at 1.8 K; **1** and **2** exhibit the highest coercive fields among all known $[Mo^{III}(CN)_7]$-based assemblies, 5000 and 4500 Oe respectively. The coercivity of **1**-**4** is correlated with the geometry of the heptacyanomolybdate(III) anion and the cyanide bridging pattern. A paramagnetic analogue of compound **1**, $\{[Mn^{II}(imH)_2]_2[Mn^{II}(H_2O)(imH)_3][Mn^{II}(imH)_4][Re^{III}(CN)_7]_2{\cdot}6H_2O\}_n$ (**1Re**), where the heptacyanomolybdate(III) anion is substituted by the diamagnetic heptacyanorhenate(III) anion is also reported which constitutes the first example of a coordination framework based on $[Re^{III}(CN)_7]^{4-}$.

Introduction

Magnetic coordination frameworks trace their origins to the discovery of Prussian Blue (PB) in 1706 in Berlin by the paint maker Diesbach while working in the laboratories of Dippel.[1] The magnetic properties of PB were first investigated in Bell laboratories by Holden et al. who reported it to be a "new low-temperature ferromagnet"[2] with a Curie temperature of 5.5 K. The mechanism of the ferromagnetic interactions in PB was identified as 'valence delocalisation'[3] in agreement with the fact that it is a class II mixed valence compound according to the Robin-Day classification.[4] Recent interest in this type of magnetic solid, has been fueled by the discovery of hexacyanometallate PB analogues that exhibit remarkably high magnetic ordering temperatures including $[Cr^{III}(CN)_6]$-based frameworks that are magnets above room temperature.[5-7]

In addition to octahedral homoleptic cyanometallates, hepta- and octacyanometallates[8,9] of 4*d* and 5*d* metal ions are important targets for a host of materials. An excellent example of this chemistry is the elaboration of magnetic frameworks of the type $\{[Mn^{II}(L)_x(H_2O)_y]_2[Mo^{III}(CN)_7]\}{\cdot}nH_2O$ (L = ligand) which were found to exhibit substantial magnetic anisotropy[10-13] owing to the geometry of the seven-coordinate pentagonal bipyramidal Mo^{III} ion. Since this pioneering work of Kahn and coworkers, numerous extended coordination assemblies based on the $[Mo^{III}(CN)_7]^{4-}$ anion have been reported,[14-22] including examples that exhibit porosity[21-22] and chirality.[22] Research efforts also have been directed at capitalizing on the magnetic anisotropy of $[Mo^{III}(CN)_7]^{4-}$ for the design of discrete polynuclear molecules.[23-25] The most exciting result in this vein is the linear $Mn^{II}_2Mo^{III}$ trinuclear molecule which exhibits the highest spin reorientation barrier among all cyanide-bridged single molecule magnets.[24-25] This remarkable SMM behaviour,[26] including hysteresis at temperatures up to 3.2 K, is attributed to anisotropic superexchange interactions between metal spin centers in the Mo^{III}-CN-Mn^{II} linkage.[27-30] which is also operative in the extended structures of $[Mo^{III}(CN)_7]^{4-}$ that exhibit wide magnetic hysteresis loops.[20,31]

Herein we report four new Mn^{II}-Mo^{III} 3-D ferrimagnetically ordered coordination frameworks exhibiting large magnetic anisotropies. The compounds $\{[Mn^{II}(imH)_2]_2[Mn^{II}(H_2O)(imH)_3][Mn^{II}(imH)_4][Mo^{III}(CN)_7]_2{\cdot}6H_2O\}_n$ (**1**) (imH = imidazole), $\{[Mn^{II}(H_2O)_2(imH)]_3[Mn^{II}(H_2O)(imH)_2][Mo^{III}(CN)_7]_2{\cdot}5H_2O\}_n$ (**2**), $\{[Mn^{II}(Htrz)(H_2O)_2][Mn^{II}(Htrz)_{0.7}(H_2O)_{2.3}][Mo^{III}(CN)_7]{\cdot}5.6H_2O\}_n$ (**3**) (Htrz = 1,2,4-triazole) and $\{[Mn^{II}(H_2O)_2]_3[Mn^{II}(H_2O)_4][Mo^{III}(CN)_7]_2{\cdot}6H_2O{\cdot}2urea\}_n$ (**4**) were prepared and fully characterized. Compounds **1** and **2** are particularly notable in that they exhibit the largest coercive fields among heptacyanomolybdate(III) containing frameworks.

[a] Faculty of Chemistry, Jagiellonian University, Gronostajowa 2, 30-387 Kraków, Poland. Email: dawid.pinkowicz@uj.edu.pl
[b] Department of Chemistry, Texas A&M University, College Station, Texas 77843, USA. E-mail: dunbar@chem.tamu.edu

† Footnotes relating to the title and/or authors should appear here.
Electronic Supplementary Information (ESI) available: additional structural diagrams and plots with PXRD, IR, and magnetic data . See DOI: 10.1039/x0xx00000x. CCDC 1899234-1899238 contain the supplementary crystallographic data for this paper which can be obtained free of charge from the Cambridge Crystallographic Data Centre via www.ccdc.cam.ac.uk/data_request/cif.

Experimental Section

Synthetic procedures

All manipulations were performed in a glovebox under an argon atmosphere unless stated otherwise. The precursor $K_4[Mo^{III}(CN)_7]\cdot 2H_2O$ was prepared by a modified procedure described in the literature[32] starting from $MoCl_3(THF)_3$ instead of K_3MoCl_6. Distilled water was deoxygenated by refluxing for 12 hours under an argon atmosphere. All other reagents were analytical grade as supplied from commercial sources (Sigma-Aldrich, Alfa Aesar, Acros Organics).

$K_4[Re^{III}(CN)_7]\cdot 2H_2O$

The compound was prepared according to a modified literature procedure.[33] Under ambient conditions, KCN (4.00 g, 61.0 mmol) was dissolved in 10 mL of H_2O which had not been deoxygenated and $ReCl_3$ (0.59 g, 2.0 mmol) was added slowly and the solution was stirred for 2 hours in air. The solution was then refluxed for 12 hours under a constant flow of argon, resulting in a brown mixture that was sealed under argon and filtered to remove a purple impurity. The mixture was then treated dropwise with 15 mL of deoxygenated methanol which produced a yellowish solid. After filtration, a creamy-yellow solid was collected and dried for 15 minutes under vacuum. Yield: 0.88 g (75%). EA Found: C, 14.69; H: 1.03; N, 17,15; calculated for $K_4[Re^{III}(CN)_7]\cdot 2H_2O$: C, 14.99; H: 0.72; N: 17.48. IR (cm^{-1}): 3613s, 3569m, 3500m, 3430m(br), 3222w, 2125m, 2113m, 2101s, 2092vs, 2070s, 2039vs, 2004m, 1627m. (Figures S1 and S2 in the ESI).

$\{[Mn^{II}(imH)_2]_2[Mn^{II}(H_2O)(imH)_3][Mn^{II}(imH)_4][Mo^{III}(CN)_7]_2\cdot 6H_2O\}_n$ (**1**). Anhydrous $MnCl_2$ (32 mg, 0.25 mmol) and imidazole (360 mg, 5.29 mmol) were dissolved in 20 mL of H_2O and added dropwise to a solution of $K_4[Mo^{III}(CN)_7]\cdot 2H_2O$ (34 mg, 0.07 mmol) in 20 mL of H_2O. Over the course of 12 h, large green needle crystals formed and were collected by decanting the solution. Yield: 30 mg (52%). EA Found: C, 34.49; H, 3.38; N, 30.71; Calculated for $[Mn^{II}(imH)_2]_2[Mn^{II}(H_2O)(imH)_3][Mn(imH)_4][Mo^{III}(CN)_7]_2\cdot 6H_2O$: C, 34.20; H, 3.54; N, 30.54. IR (cm^{-1}): 3402s, 3231s(br), 3140s, 3067m, 2956m, 2864m, 2160w, 2113s, 2050m, 1621m(br), 1537m, 1489m, 1423m, 1326m, 1257m, 1166w, 1134w, 1098w, 1065s. (Figure S3a in the ESI).

$\{[Mn^{II}(H_2O)_2(imH)]_3[Mn^{II}(H_2O)(imH)_2][Mo^{III}(CN)_7]_2\cdot 5H_2O\}_n$ (**2**)

Samples of anhydrous $MnCl_2$ (28 mg, 0.22 mmol) and imidazole (50 mg, 0.74 mmol) were dissolved in 12 mL of H_2O and the solution was added dropwise to $K_4[Mo^{III}(CN)_7]\cdot 2H_2O$ (24 mg, 0.05 mmol) in 8 mL of H_2O. After several hours, green prism crystals had formed and were collected by decantation. Yield: 10 mg (30%). EA Found: C, 26.55; H, 2.99; N, 25.63; Calculated for $[Mn^{II}(H_2O)_2(imH)]_3[Mn^{II}(H_2O)(imH)_2[Mo^{III}(CN)_7]_2\cdot 5H_2O$: C, 26.14; H, 3.33; N, 25.23; Small discrepancies between the predicted and observed composition are attributed to partial loss of water of crystallization. IR (cm^{-1}): 3601s, 3373vs(br), 3138s, 2143m, 2113s, 2094s, 1615m(br), 1533w, 1509w, 1490w, 1422w, 1327w, 1255w, 1164w, 1128w, 1098w, 1068s. (Figure S3b).

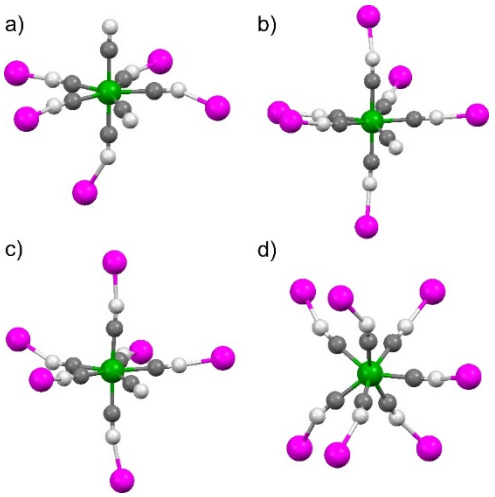

Figure 1. Heptacyanomolybdate(III) coordination environment in compounds **1**-**4** (a-d respectively); Mo – green, Mn – magenta, C – grey, N – white.

$\{[Mn^{II}(Htrz)(H_2O)_2][Mn(Htrz)_{0.7}(H_2O)_{2.3}][Mo^{III}(CN)_7]\cdot 5.6H_2O\}_n$ (**3**)

Quantities of anhydrous $MnCl_2$ (21 mg, 0.17 mmol) and 1,2,4-triazole (67 mg, 0.97 mmol) were dissolved in 6 mL of H_2O and added dropwise to a solution of $K_4[Mo^{III}(CN)_7]\cdot 2H_2O$ (24 mg, 0.05 mmol) in 6 mL of H_2O. A green precipitate formed after several hours which redissolved; large dark-green blocks crystallized within three days which were collected by decantation. Yield: 15 mg (44 %). EA Found: C, 20.76; H, 2.85; N, 28.53; Calculated for $\{[Mn^{II}(Htrz)(H_2O)_2][Mn^{II}(Htrz)_{0.7}(H_2O)_{2.3}][Mo^{III}(CN)_7]\cdot H_2O\}_n$: C, 20.78; H, 2.62; N, 28.22; Crystals of **3** lose water instantaneously when removed from the mother liquid which leads to a major difference between the number of interstitial H_2O molecules located by the X-ray data and the number calculated from the EA. IR (cm^{-1}): 3606s, 3378s(br), 2143m, 2216s, 2081s, 1615m(br), 1377w, 1297w, 1159w, 1068w, 988w (Figure S3c).

$\{[Mn^{II}(H_2O)_2]_3[Mn^{II}(H_2O)_4][Mo^{III}(CN)_7]_2\cdot 6H_2O\cdot 2urea\}_n$ (**4**)

Anhydrous $MnCl_2$ (92 mg, 0.73 mmol) and urea (350 mg, 5.83 mmol) were dissolved in 7 mL of H_2O and added dropwise to a solution of $K_4[Mo^{III}(CN)_7]\cdot 2H_2O$ (42 mg, 0.09 mmol) and urea 420 mg, 7.00 mmol) in 6.5 mL of H_2O. Large green columnar crystals appeared after 12 h and were collected by decantation. Yield: 25 mg (47%). EA Found: C, 16.01; H: 3.31; N, 21.02; Calculated for $[Mn^{II}(H_2O)_2]_3[Mn^{II}(H_2O)_4][Mo^{III}(CN)_7]_2\cdot 6H_2O\cdot 2$urea: C, 16.23; H, 3.40; N, 21.29. IR (cm^{-1}): 3485vs, 3374vs, 3340vs(br), 2139m, 2115m, 2084vs, 2060s, 1621s, 1558m, 1489m, 1136w (Figure S3d).

$\{[Mn^{II}(imH)_2]_2[Mn^{II}(H_2O)(imH)_3][Mn^{II}(imH)_4][Re(CN)_7]_2\cdot 6H_2O\}_n$ (**1Re**)

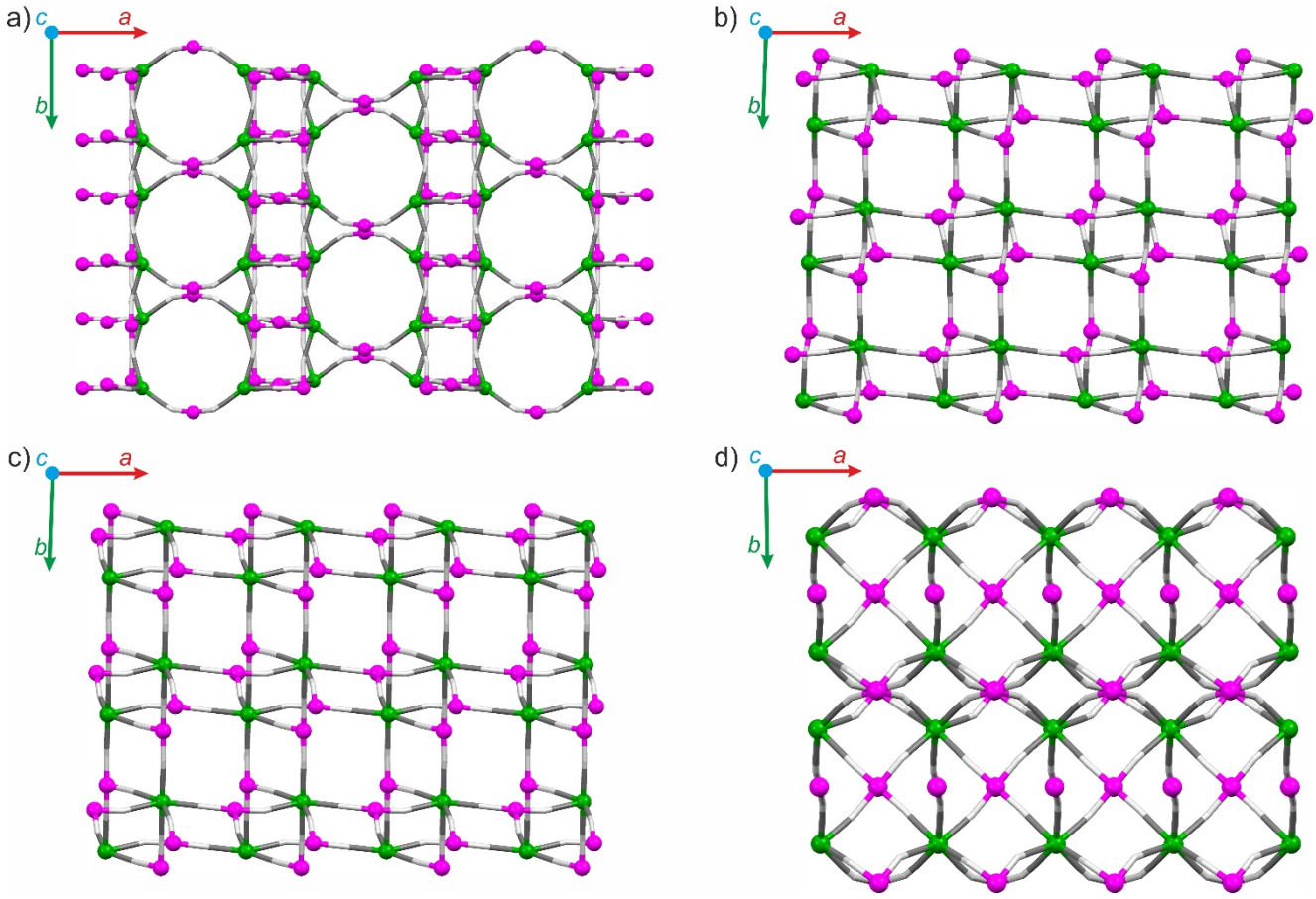

Figure 2. Coordination skeletons of compounds a) **1**, b) **2**, c) **3** and d) **4** along the *c* axis. Organic ligands, water molecules and non-bridging cyanides were omitted for the sake of clarity. Mo – green, Mn – magenta, C – grey, N – white.

Anhydrous $MnCl_2$ (32 mg, 0.25 mmol) and imidazole (360 mg, 5.29 mmol) were dissolved in 20 mL of H_2O and added dropwise to a solution of $K_4[Re^{III}(CN)_7]\cdot 2H_2O$ (41 mg, 0.07 mmol) in 20 mL of H_2O. Large dark yellow needles formed over the period of 12 h and were collected by decantation. Yield: 30 mg (47%). EA Found: C, 31.26; H, 2.95; N, 27.91; Calculated for $[Mn^{II}(imH)_2]_2[Mn^{II}(H_2O)(imH)_3][Mn^{II}(imH)_4][Re^{III}(CN)_7]_2\cdot 6H_2O$: C, 30.82; H, 3.19; N, 27.53. The small discrepancy between predicted and observed values is attributed to partial loss of water of crystallization. The purity of the sample was also confirmed by powder X-ray diffraction (Figure S5 in the ESI). IR (cm^{-1}): 3607s, 3406vs, 3140vs(br), 2956vs, 2852vs, 2711s, 2617s, 2547m, 2508m, 2382w, 2321w, 2146s, 2119vs, 2095vs, 2055vs, 1618s(br), 1532s, 1491s, 1420s, 1324s, 1282w, 1259s, 1205w, 1173m, 1158w, 1141m, 1127w, 1102s, 1089s, 1060vs (Figure S4).

Results and discussion

Crystal structures

$\{[Mn^{II}(imH)_2]_2[Mn^{II}(H_2O)(imH)_3][Mn^{II}(imH)_4][Mo^{III}(CN)_7]_2\cdot 6H_2O\}_n$ (**1**). Compound **1** crystallises in the centrosymmetric monoclinic *C*2/*c* space group with the asymmetric unit consisting of one Mo^{III} ion and three types of Mn^{II} centres, with Mn1 lying on a *c* glide plane and the Mn3 atom residing on a two-fold symmetry axis (see Figure S6 in the ESI). The Mn1 atom is bound to four imidazole equatorial ligands and two axial N-bonded CN^- groups, resulting in a slightly distorted octahedron. The Mn2 centre adopts a distorted trigonal bipyramidal geometry with two imidazole and three cyanide ligands. The Mn3 site is similar to that of Mn1, but with one imidazole ligand being substituted by a coordinated water molecule.

The $[Mo^{III}(CN)_7]^{4-}$ anion in **1** adopts a nearly ideal pentagonal bipyramidal geometry and engages in one axial and four equatorial cyanide bridges to the Mn ions (Figure 1a). Three equatorial bridges are very similar, with Mo1-Mn2 separations ranging from 5.433 Å to 5.454 Å, whereas Mo1-Mn3 and axial Mo1-Mn1 distances are significantly shorter (5.316 Å and 5.331 Å respectively) which is ascribed to the more pronounced bending of the C-N-Mn units. These structural features result in a complex 3-D coordination network. Along the *c* crystallographic axis, the bonding pattern involves square-like and circular motifs which lead to the appearance of tubular channels along the *c* axis (Figure 2a) which are occupied by water molecules.

$\{[Mn^{II}(H_2O)_2(imH)]_3[Mn^{II}(H_2O)(imH)_2][Mo^{III}(CN)_7]_2\cdot 5H_2O\}_n$ (**2**). The crystal structure of compound **2** was solved in the $P\bar{1}$ space group with two inequivalent Mn^{II} sites residing in the

asymmetric unit (Figure S7 in the ESI). The coordination sphere of one of the Mn atoms is composed of an imidazole molecule, two H_2O ligands in a *cis* geometry and three nitrogen atoms in a *mer* arrangement belonging to cyanide ligands from different $[Mo^{III}(CN)_7]^{4-}$ anions. The octahedral geometry of this centre is substantially distorted as evidenced by the O-Mn-O angle of 74.4(4)°). The second Mn^{II} center is similar to the first one, but one of its coordination sites is equally occupied by an *aqua* ligand plus one crystallization water molecule or an imidazole ligand. This disorder is likely due to scrambling of $[Mn^{II}(H_2O)_2(imidazole)]$ and $[Mn^{II}(H_2O)(imidazole)_2]$ moieties in the Mn2 position which means that the unit cell lacks inversion centre symmetry and pairs of symmetry equivalent Mn2 sites do not consist of two identical moieties.

The $[Mo^{III}(CN)_7]^{4-}$ anion in **2** is in a distorted pentagonal bipyramidal geometry (Figure 1b). with six of the seven cyanide ligands engaged in bridging interactions with Mn^{II} centres. This leads to the formation of a 3-D crossed-ladder topology (Figure 2b), similar to the $\{[Mn^{II}(H_2O)_2(imH)]_2[M^{IV}(CN)_8]\cdot 4H_2O\}_n$ networks based on octacyanometallates (M = Nb,[34] Mo,[35] W[36]) in spite of the higher imidazole content. Appearance of a structural disorder involving the additional imidazole molecule in **2** is likely related to the "missing cyanide" of the $[Mo^{III}(CN)_7]^{4-}$ as compared to the analogous $[M^{IV}(CN)_8]^{4-}$ compounds.[34-36]

$\{[Mn^{II}(Htrz)(H_2O)_2][Mn(Htrz)_{0.7}(H_2O)_{2.3}][Mo^{III}(CN)_7]\cdot 5.6H_2O\}_n$ (**3**). Compound **3** crystallizes in the $P\bar{1}$ space group. The asymmetric unit is composed of two Mn^{II} cations and one $[Mo^{III}(CN)_7]^{4-}$ anion (Figure S8 in the ESI). Mn1 is connected to three nitrogen atoms of $[Mo^{III}(CN)_7]^{4-}$ in a *mer* configuration and two oxygen atoms of H_2O ligands in a *trans* disposition. The coordination sphere is completed by a nitrogen atom from a disordered 1,2,4-triazole molecule. The best refinement was obtained for a ligand occupancy of 70%, with the remaining 30% corresponding to three hydrogen-bonded water molecules, one of which is coordinated to Mn^{II}. This composition was confirmed by elemental analysis (see Experimental section). The environment of Mn2 is similar to Mn1 except the coordinated H_2O molecules are *cis* to each other and there is no disorder associated with the 1,2,4-triazole ligand.

The $[Mo^{III}(CN)_7]^{4-}$ anion in **3** is only slightly distorted from an ideal pentagonal bipyramid (Figure 1c). As in the case of **2**, there are six cyanide bridges and one terminal equatorial cyanide which leads to nearly identical topologies (as depicted in Figure 2b and 2c). One of the equatorial Mo^{III}-C-N-Mn^{II} cyanide bridges in **3**, however, is significantly more bent at 156.7(3)° vs 174.5(5)° while both axial bridges are closer to linear as compared to **2** (**3:** 170.6(3)° and 169.3(3)° vs **2:** 163.2(5)° and 160.1(5)°; see Figure S10 in the ESI). Both networks in **2** and **3** are characterised by a loosely packed structure, rendering the crystals susceptible to water loss.

$\{[Mn^{II}(H_2O)_2]_3[Mn^{II}(H_2O)_4][Mo^{III}(CN)_7]_2\cdot 6H_2O\cdot 2urea\}_n$ (**4**)**.** Crystals of **4** belong to the $P\bar{1}$ triclinic space group with a unit cell that consists of two asymmetric units composed of $[Mo^{III}(CN)_7]^{4-}$ and four Mn^{II} centres located at special positions (Figure S9 in the ESI). Three Mn^{II} ions adopt similar coordination geometries with two *trans* H_2O ligands and four equatorially N-bonded cyanides. The fourth Mn^{II} ion is bound to four water molecules located in equatorial positions and two N atoms of *trans* CN^- ligands. The unit cell also contains six outer-sphere water molecules and two urea molecules per Mn_4Mo_2 unit. Each urea molecule is engaged in three hydrogen bonds to the carbonyl oxygen atom with the neighbouring water molecules coordinated to Mn^{II}.

Compound **4** exhibits a complex 3-D cyanide-bridged coordination network in which each heptacyanomolybdate(III) unit forms seven cyanide bridges to Mn^{II} centres. (Figure 1d). The coordination sphere of the Mo^{III} ion is intermediate between a capped trigonal prism and a capped octahedron. A fragment of the structure is depicted in Figure 2d.

The most important structural features in terms of the magnetic properties of **1-4**, namely the number of bridging cyanides and the geometry of the $[Mo^{III}(CN)_7]^{4-}$ anions, are summarized in Table 1 along with previously crystallographically determined Mn^{II}-$Mo^{III}(CN)_7$ compounds. These structural data are correlated with the temperature of the long range magnetic ordering T_c and the coercive field. Additional important crystal data and metrical parameters for compounds **1**-**4** are compiled in Table S1 and S2.

$\{[Mn^{II}(imH)_2]_2[Mn^{II}(H_2O)(imH)_3][Mn^{II}(imH)_4][Re^{III}(CN)_7]_2\cdot 6H_2O\}_n$ (**1Re**). Compound **1** and its heptacyanorhenate(III)-based analogue **1Re** are isomorphous (see structural diagrams in Figure S11 and the powder X-ray diffraction patterns in Figure S5). Stronger π-backbonding for the d^4 $[Re^{III}(CN)_7]^{4-}$ anion as compared to the d^3 $[Mo^{III}(CN)_7]^{4-}$ analogue leads to a shortening of the average M-C distance from 2.141(15) Å for Mo^{III} to 2.094(16) Å for Re^{III}. There is only a small difference in the average Mn-N bond distances in **1Re** (2.21(3) Å) and **1** (2.19(2) Å). The C-N-Mn angles (Table S2) are also similar in both compounds. Average M···Mn distances are 5.39(6) Å for **1** and 5.35(5) Å for **1Re**, an indication that the framework adjusts to the varying sizes of the heptacyanometallate units rendering it adequate for diamagnetic dilution.

Table 1. Selected structural and magnetic data for Mn^{II}-$[Mo^{III}(CN)_7]$ assemblies.

Compound[a]	No. of cyanide bridges formed by Mn(II)	No. of cyanide bridges formed by $[Mo^{III}(CN)_7]^{4-}$ Axial	Equatorial	Geometry of $[Mo^{III}(CN)_7]^{4-}$	T_c (K)	H_c (Oe)[b]	Ref.
1	2,2,3	1	4	PBPY[i]	29	$5000^{(1.8\ K)}$	This
2	3	2	4	PBPY	45	$4500^{(1.8\ K)}$	work
$(NH_4)_3[(H_2O)Mn_3(HCOO)][Mo(CN)_7]_2{\cdot}4H_2O$	4,5,5	2	5	JPBPY[j]	70	$1500^{(2\ K)}$	20
$[Mn(dpop)]_2[Mo(CN)_7]{\cdot}2H_2O$[c]	2	1	2	PBPY	5.6	$1150^{(2\ K)}$	31
Mn_2(3-pypz)$(H_2O)(CH_3CN)[Mo(CN)_7]$[d]	3,4	7		CTPR[k]	64	$820^{(2\ K)}$	37
3	3	2	4	PBPY	45	$710^{(1.8\ K)}$	This work
$[Mn(dpop)]_2[Mo(CN)_7]{\cdot}2H_2O$[c]	2	2	2	PBPY	25	$305^{(1.8\ K)}$	38
$[Mn(dpop)]_3[Mn(dpop)(H_2O)][Mo(CN)_7]_2{\cdot}13.5H_2O$[c]	1,2	1,2	2,2	PBPY	3	$90^{(1.8\ K)}$	
$[N(CH_3)_4]_2[Mn(H_2O)]_3[Mo(CN)_7]_2{\cdot}2H_2O$	4	6		COC[l]	86	$200^{(1.8\ K)}$	15
$[Mn(HL)(H_2O)]_2Mn[Mo(CN)_7]_2{\cdot}2H_2O$[e]	4	6		COC	85	$150^{(2\ K)}$	22
Mn_2(pyim)$(H_2O)(CH_3CN)[Mo(CN)_7]$[f]	3,4	7		CTPR	62	$146^{(2\ K)}$	37
$K_2Mn_3(H_2O)_6[Mo(CN)_7]_2{\cdot}6H_2O$[b]	4	7		CTPR	39	$125^{(5\ K)}$	14
4	2,4,4,4	7		CTPR/COC	59	$110^{(1.8\ K)}$	This work
Mn_2(1-pypz)$(H_2O)(CH_3CN)[Mo(CN)_7]$[g]	3,4	7		CTPR	66	$72^{(2\ K)}$	37
$[Mn_2(tea)Mo(CN)_7]{\cdot}H_2O$[h]	3,4	7		CTPR	75	$70^{(5\ K)}$	17
$K_2(H_2O)_4Mn_5(H_2O)_8(MeCN)[Mo(CN)_7]_3{\cdot}2H_2O$	3,4,4,4,5	7,6,7		PBPY/CTPR	61	$70^{(2\ K)}$	21
$Mn_2[Mo(CN)_7](pyrimidine)_2{\cdot}2H_2O$	3,4	7		COC	47	$60^{(2\ K)}$	19
$[Mn(dpop)]_4[(dpop)Mn(H_2O)]_2[Mo(CN)_7]_3{\cdot}27H_2O\}_n$[b]	1,2	2,2,2	0,2,2	PBPY	2.2	$30^{(1.8\ K)}$	39
$[NH_4]_2Mn_3(H_2O)_4[Mo(CN)_7]_2{\cdot}4H_2O$	4,5,5	7		COC/CTPR	53	$0^{(1.\ 8K)}$	18
$Mn_2(H_2O)_5[Mo(CN)_7]{\cdot}4H_2O$ (α phase)[m]	3,4	7		CTPR	51	$0^{(5\ K)}$	11
$Mn_2(H_2O)_5[Mo(CN)_7]{\cdot}4.75H_2O$ (β phase)[m]	3,4	7		CTPR	51	$0^{(5\ K)}$	12

[a]all assemblies represent 3-D connectivity except $K_2Mn_3(H_2O)_6[Mo(CN)_7]_2{\cdot}6H_2O$ and $[Mn(dpop)]_4[(dpop)Mn(H_2O)]_2[Mo(CN)_7]_3{\cdot}27H_2O\}_n$, [b]values listed in brackets represent temperatures at which hysteresis loops were recorded, [c]dpop = 2,13-dimethyl-3,6,9,12,18-pentaazabicyclo[12.3.1]-octadeca-1(18),2,12,14,16-pentaene), [d]3-pypz = 2-(1H-pyrazol-3-yl)pyridine, [e]L = *N*,*N*-dimethylalaninol, [f]pyim = 2-(1H-imidazol-2-yl)pyridine, [g]1-pypz = 2-(1H-pyrazol-1-yl)pyridine, [h]tea = triethanolamine, [i]PBPY = pentagonal bipyramid, [j]JPBPY = Johnson pentagonal bipyramid, [k]CTPR = capped trigonal prism, [l]COC = capped octahedron, [m]while authors report both phases to be distorted pentagonal bipyramids, quantitative estimation of geometry using SHAPE software[40] leads to the distorted capped trigonal prism

Magnetic properties

Compounds **1**-**4** are paramagnetic at temperatures higher than 29 K (**1**), 45 K (**2** and **3**) and 59 K (**4**). Experimental values of χT versus T at 250 K are 8.94 cm^3 K mol^{-1} for **1**, 9.14 cm^3 K mol^{-1} for **2**, 9.04 cm^3 K mol^{-1} for **3** and 8.96 cm^3 K mol^{-1} for **4** (see Figure S12 in the ESI), which are close to the expected spin-only value of 9.13 cm^3 K mol^{-1} per Mn_2Mo formula unit. Small discrepancies are attributed deviations of the *g* factor of Mo^{III} from 2.0[41] and antiferromagnetic interactions between Mo^{III} and Mn^{II} spin centers.

Compounds **1**-**4** exhibit a magnetic phase transition to a ferrimagnetic state as evidenced by an abrupt increase of the FC (field-cooled) magnetization and bifurcation of the ZFC/FC (zero field-cooled/field-cooled) at the critical temperatures of 29 K for **1**, 45 K for **2** and **3** and 59 K for **4** (Figure 3). These T_c values are in accord with the position of the χ' peak in the AC (alternating current) molar magnetic susceptibility data (Figure S13a-d). The higher T_c values across the series are consistent with the increasing number of bridging cyanides per $[Mo^{III}(CN)_7]^{4-}$ moiety (see Table 1 for reference). It is noted that compounds **2** and **3** with identical crossed-ladder topologies order magnetically at the same temperature of 45 K.

The *M*(*H*) curves for all four compounds exhibit magnetic hysteresis at 1.8 K (Figure 4 and Table 1). In the case of **1**, the coercive field (H_c) is 5000 Oe with a remnant magnetisation M_r of 3.8 Nβ and for **2** H_c = 4500 Oe and M_r = 4.3 Nβ. For **3** and **4** the hysteresis loops are narrower at 710 and 110 Oe and the remnant magnetization values are 3.6 and 1.2 Nβ, respectively. Of particular note is the fact that **1** and **2** exhibit coercivities of 5000 and 4500 Oe, respectively which are the largest reported values for heptacyanomolybdate(III) containing compounds. The H_c values are independent of the grain shape or size as the samples of **1**-**4** are all crystalline (0.2 mm monocrystals) with no visible grain boundaries, in contrast to metal alloys or ceramic magnets produced by sintering of metal oxides. Given the absence of other magnetically anisotropic building blocks, the coercivity properties of $\{[Mn^{II}(L)_x(H_2O)_y]_2[Mo^{III}(CN)_7]\}{\cdot}nH_2O$ magnets emanate from the orbitally degenerate S = ½ pentagonal bipyramidal $[Mo^{III}(CN)_7]^{4-}$ anion which engages in

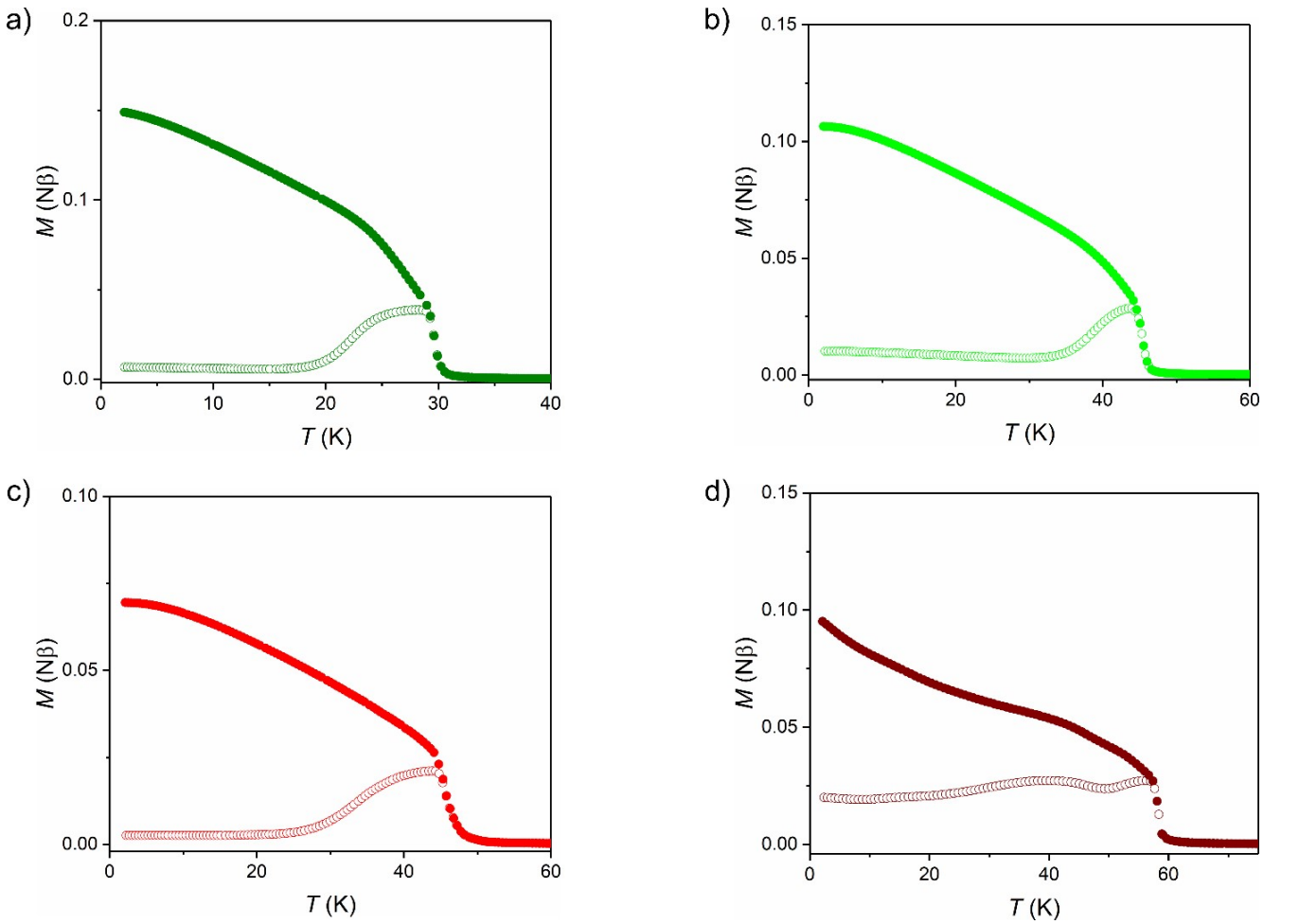

Figure 3. Zero field-cooled (open circles) and field-cooled (full circles) $M(T)$ plots for compounds **1**-**4** (a-d respectively) at H_{DC} = 3 Oe.

anisotropic exchange interactions.[27-30] The widest magnetic hysteresis loop was observed for **1** whose structure is closest to an ideal pentagonal bipyramid (PBP) (see Table S1). One might expect **3** to exhibit the coercivity similar to **1** given that the Mo^{III} unit is only slightly more distorted from pentagonal bipyramidal geometry, but the H_c value is only 710 Oe as compared to 5000 Oe for **1**. In addition, this value is actually seven times less than that of **2** (4500 Oe) in spite of the fact that the $[Mo^{III}(CN)_7]^{4-}$ anion in **2** is significantly more distorted from an ideal PBP. The main structural differences between **2** and **3** are less bent apical C-N-Mn angles in **3** and a significant bending of the equatorial C-N-Mn bridge in **3** (156.7(3)°) as compared to **2** (174.5(5)°; Figure S10 and Table S2 in the ESI). These metrical differences directly impact orbital overlap hence magnetic exchange interactions as well as orientations of the anisotropy axis associated with the $[Mo^{III}(CN)_7]^{4-}$ moiety.[30]

The coercive field of 110 Oe exhibited by **4** indicates a small magnetic anisotropy, typical of heptacyanomolybdate(III) assemblies with large deviations from a pentagonal bipyramidal geometry. An analysis of the coercivities and the geometry of the $[Mo^{III}(CN)_7]^{4-}$ bridging unit for the compounds in Table 1 reveals that a pentagonal bipyramidal geometry is a necessary, but not sufficient, criterion for wide magnetic hysteresis loops.

The $M(H)$ curves at 7 T reach values of 7.55 Nβ for **1**, 8.10 Nβ for **2**, 8.99 Nβ for **3** and 8.98 Nβ for **4**, approaching the expected 9.0 Nβ for antiferromagnetically coupled Mn_2Mo units. It is worth mentioning the magnetization data for **1** and **2** do not saturate (Figure S14 in the ESI) which is another indication of substantial magnetic anisotropy, as even a strong magnetic field of 7 T is insufficient to completely align magnetic domains.

Given its large H_c value, compound **1** is a good candidate for introducing SMM-like behaviour via diamagnetic dilution using $[Re^{III}(CN)_7]^{4-}$. Our attempt to synthesize the structural analogue of **1** was successful and led to the isolation of $\{[Mn^{II}(imH)_2]_2[Mn^{II}(H_2O)(imH)_3][Mn^{II}(imH)_4][Re^{III}(CN)_7]_2{\cdot}6H_2O\}_n$ (**1Re**). The compound is a simple paramagnet with very weak antiferromagnetic interactions between the Mn^{II} ions, separated by the diamagnetic Re^{III} centers. The magnetic data were modelled to the mean-field approximation using PHI software,[42] and fitting of $\chi T(T)$ curve was performed with the following expression:

$$\chi = \chi_{calc}/[1-(zJ/N_A\mu_B^2)\chi_{calc}] \quad \text{(Eq. 1)}$$

which yields g_{Mn} = 2.02(5) and zJ = -0.05(1) cm^{-1} (Figure S15 in the ESI). The magnetization data at 7 T and 2 K approach 9.90 Nβ which is very close to the expected spin-only value of 10 Nβ. Likewise, the χT value of 8.86 cm^3 K mol^{-1} at 250 K is in accord with the expected 8.75 cm^3 K mol^{-1} value for two non-

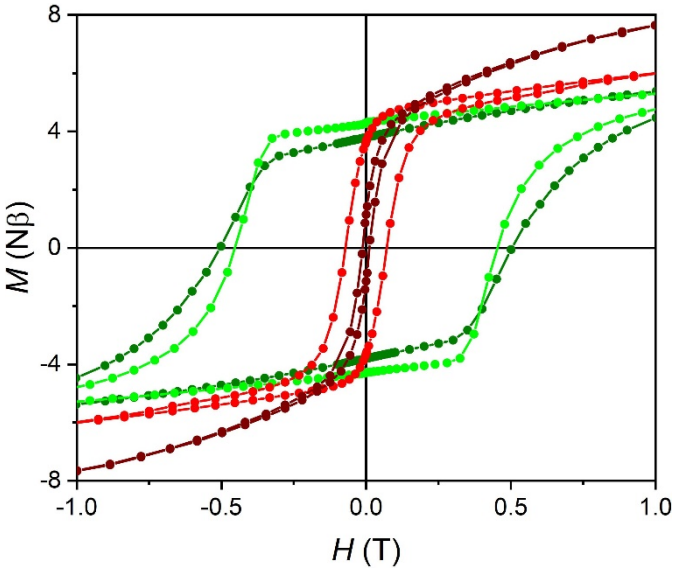

Figure 4. Magnetisation versus magnetic field plots for compounds **1** (dark green), **2** (green), **3** (red) and **4** (dark red) at T = 1.8 K. Solid lines are guides for the eye.

interacting g = 2.0 Mn^{II} centres. The decrease in χT vs T below 20 K is attributed to weak antiferromagnetic interactions through the diamagnetic $[Re^{III}(CN)_7]^{4-}$ linker. AC magnetic susceptibility measurements for this compound did not reveal any out-of-phase signal down to 1.8 K. Synthesis of mixed Mo^{III}/Re^{III} systems based on these findings is in progress.

Conclusions

Four new 3-D coordination networks based on Mn^{II} units and $[Mo^{III}(CN)_7]^{4-}$ were obtained and their magnetic ordering temperatures and coercivities were correlated with the connectivity patterns, metrical parameters and the geometry of the heptacyanomolybdate(III) anion. The collective results support the hypothesis that the pentagonal bipyramidal geometry leads to significant magnetic anisotropy and the observation of wide magnetic hysteresis loops. Importantly, it was found that the presence of equatorial cyanide bridges does not suppress magnetic hysteresis in **1-3**. Moreover, it appears that the Mn-N-C angles in **1-4** are important for obtaining hard magnetic materials with $[Mo(CN)_7]^{4-}$ building blocks, although the current study is too limited to allow for specific conclusions in this regard.

Reactions of the diamagnetic $[Re^{III}(CN)_7]^{4-}$ anion[43] that involve substitution of $[Mo^{III}(CN)_7]^{4-}$ in $\{[Mn^{II}(L)_x(H_2O)_y]_2[Mo^{III}(CN)_7]\}\cdot nH_2O$ compounds are promising avenues of investigation as evidenced by the fact that the 3-D Mn^{II}-$[Re^{III}(CN)_7]$ analogue, **1Re**, was successfully isolated in this study. This paramagnetic framework solid, the first example of a bimetallic coordination framework based on the heptacyanorhenate(III) anion, is isomorphous to its ferrimagnetically ordered heptacyanomolybdate(III) analogue, a fact that bodes well for the goal of pursuing magnetic dilution of the Mn^{II}-Mo^{III} networks.[44] Partial, rather than complete, substitution of the paramagnetic heptacyanomolybdate(III) anion in these networks could lead to SMM-like slow paramagnetic relaxation, as, for example, in lanthanide-based networks[45-46] such as $Dy_{0.06}Y_{0.94}(OH)CO_3$ which exhibits a spin-reversal barrier as high as 196(6) K in a zero DC field.[47] Analogous studies for transition metal-based frameworks are not known, however, and are worth pursuing; work in this vein is in progress.

Conflicts of interest

There are no conflicts to declare.

Acknowledgements

This work was financed by the Polish National Science Centre within the Sonata Bis 6 (2016/22/E/ST5/00055) research project. KRD is grateful to the National Science Foundation (CHE-1808779) and the Robert A. Welch Foundation under Grant Number A-1449 for financial support.

Notes and references

1 A. Kraft, *Bull. Hist. Chem.*, 2008, **33**, 61–67
2 A. N. Holden, B. T. Matthias, P. W. Anderson, H. W. Lewis, *Phys. Rev. B*, 1956, **102**, 1463
3 B. Mayoh, P. Day, *Chem. Soc., Dalton Trans.*, 1976, 1483-1486
4 M. B. Robin, P. Day, *Adv. Inorg. Chem. Radiochem.*, 1968, **10**, 247
5 B. Sieklucka, D. Pinkowicz, *Molecular Magnetic Materials: Concepts and Applications*, Wiley 2017
6 S. Ferlay, T. Mallah, R. Ouahès, P. Veillet, M. Verdaguer, *Nature*, 1995, **378**, 701
7 S. M. Holmes, G. S. Girolami, *J. Am. Chem. Soc.*, 1999, **121**, 5593
8 B. Sieklucka, R. Podgajny, P. Przychodzeń, T. Korzeniak, *Coord. Chem. Rev.*, 2005, **249**, 2203
9 Y. Arimoto, S.-I. Ohkoshi, Z. J. Zhong, H. Seino, Y. Mizobe, K. Hashimoto, *J. Am. Chem. Soc.*, 2003, **125**, 9240
10 J. Larionova, J. Sanchiz, S. Gohlen, L. Ouahab, O. Kahn, *Chem. Commun.*, 1998, **0**, 953
11 J. Larionova, R. Clérac, J. Sanchiz, O. Kahn, S. Golhen, L. Ouahab, *J. Am. Chem. Soc.*, 1998, **120**, 13088
12 J. Larionova, O. Kahn, S. Golhen, L. Ouahab, R. Clérac, *Inorg. Chem.*, 1999, **38**, 3621
13 O. Kahn, J. Larionova, L. Ouahab, *Chem. Commun.*, 1999, **0**, 945
14 J. Larionova, O. Kahn, S. Gohlen, L. Ouahab, R. Clérac, *J. Am. Chem. Soc.*, 1999, **121**, 3349
15 J. Larionova, R. Clérac, B. Donnadieu, C. Guérin, *Chem. Eur. J.*, 2002, **8**, 2712
16 A. K. Sra, F. Lahitite, J. V. Yakhmi, O. Kahn, *Physica B*, 2002, **321**, 87
17 S. Tanase, F. Tuna, P. Guionneau, T. Maris, G. Rombaut, C. Mathonière, M. Andruh, O. Kahn, J.-P. Sutter, *Inorg. Chem.*, 2003, **42**, 1625
18 X. F. Le Goff, S. Willemin, C. Coulon, J. Larionova, B. Donnadieu, R. Clérac, *Inorg. Chem.*, 2004, **43**, 4784
19 K. Tomono, Y. Tsunobuchi, K. Nakabayashi, S.-i. Ohkoshi, *Inorg. Chem.*, 2010, **49**, 1298
20 L. Shi, D. Shao, F.-Y. Shen, X.-Q. Wei, X.-Y. Wang, *Chin. J. Chem.*, 2018, **37**, 19
21 J. Milon, P. Guionneau, C. Duhayon, J.-P. Sutter, *New J. Chem.*, 2011, **35**, 1211

22 J. Milon, M.-C. Daniel, A. Kaiba, P. Guionneau, S. Brandès, J.-P. Sutter, *J. Am. Chem. Soc.*, 2007, **129**, 13872
23 X.-Y. Wang, A. V. Prosvirin, K. R. Dunbar, *Angew. Chem. Int. Ed.*, 2010, **49**, 5081
24 K. Qian, X.-C. Huang, C. Zhou, X.-Z. You, X.-Y. Wang, K. R. Dunbar, *J. Am. Chem. Soc.*, 2013, **135**, 13302
25 D.-Q. Wu, D. Shao, X.-Q. Weri, F.-X. Shen, L. Shi, D. Kempe, Y.-Z. Zhang, K. R. Dunbar, X.-Y. Wang, *J. Am. Chem. Soc.*, 2017, **139**, 11714
26 D. Gatteschi, R. Sessoli, J. Villain, *Molecular Nanomagnets*, Oxford University Press 2006
27 V. S. Mironov, L. F. Chibotaru, A. Ceulemans, *J. Am. Chem. Soc.*, 2003, **125**, 9750
28 V. S. Mironov, *Inorg. Chem.*, 2015, **54**, 11339
29 V. S. Mironov, *Inorganics*, 2018, **6**, 58
30 L. F. Chibotaru, M. F. A. Hendrickx, S. Clima, J. Larionova, A. Ceulemans, *J. Phys. Chem. A.*, 2005, **109**, 7251
31 X.-Q. Wei, K. Qian, H.-Y. Wei, X.-Y. Wang, *Inorg. Chem.*, 2016, **55**, 5107
32 R. C. Young, *J. Am. Chem. Soc.*, 1932, **54**, 1402
33 W. P. Griffith, P. M. Kiernan, J.-M. Brégeault, *J. Chem. Soc., Dalton Trans.*, 1978, 1411
34 D. Pinkowicz, R. Podgajny, W. Nitek, M. Makarewicz, M. Czapla, M. Mihalik, M. Bałanda, B. Sieklucka, *Inorg. Chim. Acta*, 2008, **361**, 3957
35 L. Shen, Y. Zhang, J Uiu, *J. Coord. Chem.*, 2006, **59**, 629
36 M. Magott, M. Reczyński, B. Gaweł, B. Sieklucka, D. Pinkowicz, *J. Am. Chem. Soc.*, 2018, **140**, 15876
37 X.-Q. Wei, Q. Pi, F-X. Shen, D. Shao, H.-Y. Wei, X.-Y. Wang, *Dalton Trans.*, 2018, **47**, 11873
38 Q.-L. Wang, H. Southerland, J.-R. Li, A. V. Prosvirin, H. Zhao, K. R. Dunbar, *Angew. Chem. Int. Ed.*, 2012, **51**, 9321
39 Q.-L. Wang, Y.-Z. Zhang, H. Southerland, A. V. Prosvirin, H. Zhao, K. R. Dunbar, *Dalton. Trans.*, 2014, **43**, 6802
40 M. Llunell, D. Casanova, J. Cirera P. Alemany, S. Alvarez, *SHAPE v. 2.1*, 2013, University of Barcelona: Barcelona, Spain
41 G. R. Rossman, F.-D. Tsay, H. B. Gray, *Inorg. Chem.*, 1973, **12**, 824
42 N. F. Chilton, R. P. Anderson, L. D. Turner, A. Soncini, K. S. Murray, *J. Comput. Chem.*, 2013, **34**, 1164
43 P. M. Kiernan, W. P. Griffith, *Inorg. Nucl. Chem. Letters*, 1976, **12**, 377
44 P. Konieczny, R. Pełka, T. Wasiutyński, M. Oszajca, B. Sieklucka, D. Pinkowicz, *Dalton Trans.*, 2018, **47**, 11438
45 R. Giraud, W. Wernsdorfer, A. M. Tkachuk, D. Mailly, B. Barbara, *Phys. Rev. Lett.*, 2001, **87**, 057203
46 B. Monteiro, J. T. Coutinho, C. C. L. Pereira, L. C. J. Pereira, J. Marçalo, M. Almeida, J. J. Baldovi, E. Coronado, A. Gaita-Ariño, *Inorg. Chem.*, 2015, **54**, 1949
47 J. Liu, Y.-C. Chen, J.-J. Lai, Z.-H. Wu, L.-F. Wang, Q.-W. Li, G.-Z. Huang, J.-H. Jia, M.-L. Tong, *Inorg. Chem.*, 2016, **55**, 3145

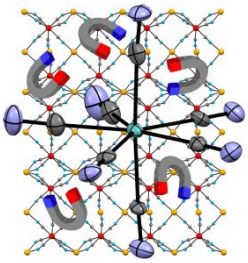

The magnetic coercivity of four new heptacyanomolybdate(III)-based coordination polymers is correlated with the geometry of the $[Mo^{III}(CN)_7]^{3-}$ anion and the cyanide bridging pattern of the framework.